Clinical and Experimental Obstetrics & Gynecology

*Clin. Exp. Obstet. Gynecol.* **2026**; 53(11): 48528
https://doi.org/10.31083/CEOG48528

*Original Research*

# MFAP5 Promotes Trophoblast Dysfunction via the Notch/EMT Axis: From Bioinformatics to Functional Validation in Preeclampsia

Jian Shen[1,2], Yu Zhen[2], Zhijian Wang[1,3,*]

[1]Department of Obstetrics and Gynecology, Nanfang Hospital, Southern Medical University, 510515 Guangzhou, Guangdong, China
[2]Department of Obstetrics and Gynecology, The Central Hospital of Wuhan, Tongji Medical College, Huazhong University of Science and Technology, 430014 Wuhan, Hubei, China
[3]Department of Obstetrics and Gynecology, The Third Affiliated Hospital, Guangzhou Medical University, 510150 Guangzhou, Guangdong, China
*Correspondence: wzjnfyy@163.com (Zhijian Wang)

Academic Editors: George Daskalakis and Michael H. Dahan
Submitted: 25 November 2025 Revised: 17 April 2026 Accepted: 8 May 2026 Published: 11 November 2026

**Abstract**

**Background:** The placenta plays a central role in the pathogenesis of preeclampsia (PE), with abnormal extracellular matrix remodelling and impaired angiogenesis representing hallmark features of the condition. Microfibril-associated protein 5 (MFAP5) is a key extracellular matrix regulator involved in vascular development; yet, its role in PE remains unexplored. Through bioinformatics screening, we identified differential MFAP5 expression in PE placentas and subsequently validated the MFAP5-PE association and elucidated its functional role in disease pathogenesis. **Methods:** Differential expression analysis was performed using the GSE10588 and GSE44711 datasets from the Gene Expression Omnibus database, leading to the identification of *MFAP5* as a co-expressed differentially expressed gene (DEG) for further validation. Protein-protein interaction partners of MFAP5 were subsequently screened using the STRING database. Gene Ontology enrichment and Kyoto Encyclopedia of Genes and Genomes pathway analyses were conducted on the candidate gene set to explore functional roles and pathway involvement. Bioinformatics findings were experimentally validated by assessing MFAP5 protein expression in normal and PE placental tissues using immunohistochemistry and western blotting (WB). The functional impact of *MFAP5* on trophoblast behavior was then evaluated in HTR8/SVneo cells using Cell Counting Kit-8, apoptosis, and scratch wound healing assays. WB was additionally employed to confirm the involvement of MFAP5 in regulating the Notch signalling pathway and epithelial-mesenchymal transition (EMT). **Results:** Differential expression analysis of the GSE10588 and GSE44711 datasets identified significantly higher *MFAP5* levels in PE placental tissues than in normotensive controls. This observation was further corroborated using an independent external dataset (GSE75010). A protein-protein interaction network analysis identified 22 experimentally validated binding partners of MFAP5. Further network expansion and analysis using GeneMANIA (Version 3.6.0, University of Toronto, Toronto, Canada) identified a broader set of associated genes, including those linked to the Notch signaling pathway. Elevated MFAP5 protein expression in PE placental tissues was experimentally confirmed by immunohistochemistry and WB. In functional assays, *MFAP5* overexpression reduced Notch pathway protein levels, suppressed proliferation, migration, and EMT in HTR8/SVneo cells, and promoted apoptosis. **Conclusions:** *MFAP5* serves as a key mediator in PE progression, with its upregulation influencing trophoblast EMT through the Notch signaling pathway. These findings highlight MFAP5 as a potential pathogenic factor and a candidate biomarker warranting further validation in the circulation as a diagnostic marker for PE.

**Keywords:** preeclampsia; differentially expressed gene; microfibril-associated protein 5

## 1. Introduction

Preeclampsia (PE) is a multisystemic disorder characterized by new-onset hypertension and proteinuria after 20 weeks of gestation, affecting approximately 2% to 8% of pregnancies worldwide [1,2]. The placenta plays an essential role during mammalian gestation, and placental impairment has been implicated in a broad range of human pregnancy-related disorders [3]. Insufficient extravillous trophoblast (EVT) invasion during early gestation is now recognized as a key factor underlying placental developmental defects that contribute to the pathogenesis of PE [4]. The differentiation of villous cytotrophoblasts into invasive EVTs is driven by epithelial-mesenchymal transition (EMT), a process essential for maternal-fetal interface formation and placental development. Disruption of EMT impairs this phenotypic switch, compromising EVT migration and invasion, and resulting in shallow placental implantation and insufficient spiral artery remodeling, hallmarks of PE [5].

The extracellular matrix (ECM) provides structural and biochemical support critical for placental development and spiral artery remodeling. Dysregulation of ECM composition is increasingly recognized in PE pathogenesis [6,7]. As a key ECM glycoprotein, microfibril-associated protein 5 (MFAP5) participates in cell-matrix interactions, affects endothelial cell function, and regulates transforming growth factor-beta (TGF-β) and Notch signaling pathways, each of which has been implicated in placental dysfunction [8,9]. However, despite its potential relevance, *MFAP5* ex-

**Copyright**: © 2026 The Author(s). Published by IMR Press.
This is an open access article under the CC BY 4.0 license.

**Publisher's Note**: IMR Press stays neutral with regard to jurisdictional claims in published maps and institutional affiliations.

pression pattern and functional significance in human PE placentas have not yet been investigated.

Microarray-based gene transcriptome analysis has been extensively applied in recent years to investigate the pathogenesis of placental-related disorders, including PE [10]. By profiling gene expression differences in PE versus normotensive placental tissues, differentially expressed genes (DEGs) can potentially be used as therapeutic targets or biomarkers. In this study, we re-analysed microarray datasets to screen for DEGs in PE and identified *MFAP5* as a consistently upregulated gene. To address this knowledge gap, subsequent bioinformatics analyses including protein-protein interaction (PPI) and enrichment studies, linked *MFAP5* to ECM organization and the Notch signalling pathway. Both ECM and Notch signaling pathway are known as critical factors of EMT in trophoblasts. Based on the premise that EMT dysregulation is central to the PE pathogenesis, we hypothesized that *MFAP5* contributes to this process through the Notch/EMT axis and aimed to validate this by using integrated bioinformatics and functional experiments.

## 2. Materials and Methods

This study employed a sequential two-phase design. In Phase 1 (Discovery & Bioinformatics Analysis), human PE datasets were retrieved from the Gene Expression Omnibus database (http://www.ncbi.nlm.nih.gov/geo/) in October 2023 [11,12]. GSE10588 (GPL2986), containing 26 controls and 17 PE cases, and GSE44711 (GPL10558), comprising 20 normotensive controls and 20 PE cases, were analysed to identify DEGs. To confirm the expression patterns observed in the discovery cohorts, the selected DEGs were further assessed in GSE75010 (GPL6244), an independent validation dataset comprising 80 PE and 77 normotensive placental samples. The details are shown in **Supplementary Table 1**. In Phase 2 (Experimental Validation), immunohistochemistry (IHC) and western blotting (WB) were used to preliminarily assess MFAP5 protein in a limited set of placental tissues. To clarify the mechanistic involvement of *MFAP5*, functional experiments were performed in HTR8/SVneo trophoblast cell line.

### *2.1 Identification of DEGs*

Separate analyses of the GSE10588 and GSE44711 datasets were conducted with the limma R package for DEG (Version 3.54.0, Melbourne, Australia). Differential expression was determined with thresholds of $p < 0.05$ and $|\log FC| > 1$. Overlapping DEGs between the two datasets were subsequently obtained using Venn diagram (Version 1.7.3, Melbourne, Australia) analysis. The selected DEG *MFAP5* was further verified in another dataset GSE75010, comprising a larger sample size.

### *2.2 PPI Network Mapping*

PPI network was retrieved from the STRING database (Version 11.5, https://string-db.org/, EMBL, Heidelberg, Germany) [13], which compiles known and predicted protein interactions. For the STRING analysis, the mapping was performed by querying "Protein name-MFAP5" with the edge type set to "evidence", active interaction sources restricted to "experiments and databases", and a maximum of 50 interactors. A minimum interaction score of 0.150 (low confidence) was used to construct the initial protein–protein interaction network to encompass a wider range of biological associations. A more stringent threshold of 0.900 (highest confidence) was further applied to extract the highest confidence interaction network. Based on this analysis, 22 MFAP5-interacting proteins were identified, with support from both experimental evidence and database records. The interaction relationships between these binding proteins and their target genes were subsequently characterized, leading to the construction of a comprehensive interaction network. To further explore co-expression patterns and functional linkages among the identified hub genes, we next utilized GeneMANIA (Version 3.6.0, https://www.genemania.org/, University of Toronto, Canada) [14].

### *2.3 Enrichment Analysis of MFAP5*

Enrichment analysis was performed using the 22 MFAP5-binding partners identified from the PPI network and GeneMANIA interaction analyses to investigate the biological roles of MFAP5. The R package "clusterProfiler" (Version 4.1.1, Guangzhou, Guangdong, China) and Metascape (Version 3.5, https://metascape.org, Sanford Burnham Prebys, San Diego, CA, USA) [15] were applied for Gene Ontology (GO) and Kyoto Encyclopedia of Genes and Genomes (KEGG) enrichment analysis, setting the significance level at $p < 0.05$ for all statistical evaluations.

### *2.4 Placental Tissue Specimens*

Placental tissues at delivery were obtained from 5 normotensive pregnant women and 5 PE patients. Upon collection, all samples were immediately frozen in liquid nitrogen and stored at –80 °C until processing [16]. Since this was an observational study, the sample size was not predetermined through statistical approaches. Inclusion criteria were as follows: PE group, (1) age 18–45 years, (2) systolic blood pressure (SBP) ≥140 mmHg or diastolic blood pressure (DBP) ≥90 mmHg presenting on at least two occasions, from 20 weeks of gestation onward; (3) proteinuria, diagnosed by either 24-hour urinary protein ≥0.3 g or a dipstick test of ≥ + on a random urine specimen; Normal group, (1) age 18–45 years, (2) healthy pregnant women. Exclusion criteria for both the PE and control groups were as follows: chronic hypertension, hepatitis, renal disease, cardiovascular disease, diabetes, any indication of infection during labour, or additional maternal and fetal complications (e.g., chromosomal abnormalities or fetal anomalies) [16]. Approval for all human tissue procedures was obtained from the Clinical Research Ethics Committee of the Central Hospital of Wuhan, and the study was con-

ducted in accordance with the approved protocol (Approval No.: WHZXKYL2023-134). The study was conducted in accordance with the Declaration of Helsinki, and written informed consent was obtained from all enrolled subjects prior to participation.

### *2.5 IHC Staining*

Placental tissue samples were initially fixed in 4% paraformaldehyde, followed by dehydration with graded ethanol, paraffin embedding, and sectioning at 5 µm. IHC detection of MFAP5 was subsequently performed on the resulting sections using a specific primary antibody (ab171737, Abcam, Cambridge, UK) and a Histostain-Plus DAB visualization kit (Mingrui Biotech, Shanghai, China), according to the manufacturer's instructions [17]. Immunohistochemical staining was evaluated independently by two investigators. Images were analyzed using Aipathwell (Servicebio, Wuhan, Hubei, China) image analysis software [18]. Aipathwell automatically located cell nuclei and defined positive regions. The integrated optical density (IOD) was calculated as the sum of optical density values of all positive pixels. The mean optical density (MOD) was calculated as MOD = IOD / positive area.

### *2.6 HTR8/SVneo Cell Culture and Transfection*

HTR8/SVneo cells (Procell Life Science & Technology, Wuhan, Hubei, China), a human EVT cell line, were kept in RPMI 1640 (Gibco, USA) with 10% fetal bovine serum (FBS) and 1% penicillin-streptomycin. Cells were cultured at 37 °C with 5% $CO_2$. Cells were transfected with pcDNA3.1-MFAP5 or an empty vector using Lipofectamine 3000 (Thermo Fisher, Waltham, MA, USA), in accordance with the manufacturer's guidelines. Cells were treated with 10 µM N-[N-(3,5-Difluorophenacetyl)-L-alanyl]-S-phenylglycine t-butyl ester (DAPT, a Notch signaling inhibitor, Selleck Chemicals) or left untreated for 24 hours, beginning 24 hours post-transfection, prior to subsequent experiments. Based on these conditions, 3 groups were established: the overexpression-negative control (OE-NC) group (transfected with empty vector), the OE-MFAP5 group (transfected with MFAP5 overexpression plasmid), and the OE-MFAP5 + DAPT group (transfected with MFAP5 overexpression plasmid followed by DAPT treatment).

### *2.7 RNA Isolation and Reverse Transcription Quantitative Polymerase Chain Reaction (RT-qPCR) Analysis*

Utilizing TRIzol reagent (Invitrogen, Carlsbad, CA, USA) in accordance with the manufacturer's instructions, total RNA was obtained from HTR8/SVneo cells in each of the 3 groups (OE-NC, OE-MFAP5, and OE-MFAP5 + DAPT). NanoDrop 2000 spectrophotometry (Thermo Fisher Scientific, USA) was used to assess RNA concentration and purity. Subsequently, reverse transcription of 1 µg of total RNA was performed using the PrimeScript RT Reagent Kit (Takara, Japan).

RT-qPCR was conducted on an ABI StepOnePlus system (Applied Biosystems, Foster City, CA, USA) using SYBR Green Premix Ex Taq (Takara, Kusatsu, Shiga, Japan). Primer sequences for MFAP5 and other genes are listed in **Supplementary Table 2**. After an initial denaturation at 95 °C for 30 s, 40 cycles of amplification were performed (95 °C for 5 s, 60 °C for 30 s). Quantification of MFAP5 mRNA was performed via the $2^{-\Delta\Delta Ct}$ approach [19], with glyceraldehyde-3-phosphate dehydrogenase (GAPDH) used for normalization. Triplicate measurements were performed for each sample across three independent experimental repeats.

### *2.8 Protein Extraction and WB Analysis*

Protein lysates were prepared from placental tissues with RIPA lysis buffer (Sigma-Aldrich, St. Louis, MO, USA). Protein samples (100 µg each) were resolved by sodium dodecyl sulfate-polyacrylamide gel electrophoresis (SDS-PAGE) and transferred to nitrocellulose membranes (Thermo, USA). The blots were then incubated overnight with anti-MFAP5 and anti-GAPDH (AF7021, Affinity Biosciences, Changzhou, China) primary antibodies, each diluted 1:1000. Following washing steps, secondary antibodies (horseradish peroxidase-conjugated goat anti-rabbit or goat anti-mouse, Santa Cruz, USA) were applied to the membranes at a 1:5000 dilution. The bands were visualized by chemiluminescence using the EasySee Western Blot Kit (TransGen Biotech, China) and then imaged with a Chemi-Doc Imaging System (Bio-Rad, USA).

From HTR8/SVneo cells of the 3 groups (OE-NC, OE-MFAP5, and OE-MFAP5 + DAPT), total protein was extracted with RIPA lysis buffer (Beyotime, China), and supplemented with protease and phosphatase inhibitors (Roche, Switzerland). Quantification of protein content was performed using a bicinchoninic acid protein assay kit (Thermo Fisher Scientific, USA). After separation by 10% SDS-PAGE, equal amounts of protein (30 µg) were transferred onto polyvinylidene fluoride (PVDF) membranes (Millipore, USA). After blocking in Tris-buffered saline with 0.1% Tween-20 (TBST) containing 5% non-fat milk for 1 hour at ambient temperature, membranes were incubated overnight at 4 °C with a primary antibody against MFAP5, N-cadherin (1:1000, A19083, Abclonal, China), E-cadherin (1:1000, A20798, Abclonal, China), zonula occludens-1 (ZO-1, 1:1000, A11417, Abclonal, China), Notch1 (1:1000, A19090, Abclonal, China), hairy/enhancer-of-split related with YRPW motif 1 (Hey1, 1:500, A16110, Abclonal, China), jagged canonical Notch ligand 1 (JAG1, 1:1000, A11733, Abclonal, China) and GAPDH. Following three washes with TBST, the membranes were probed with horseradish peroxidase-conjugated secondary antibodies (1:5000, Santa Cruz, USA) for 1 hour at room temperature. The WB bands of cell samples were captured using film exposure (Fuji film, Japan), and the exposed film was scanned using a

scanner (EPSON, Perfection V39, Japan). Signal intensities were analysed with Image J software (Version 1.54g, NIH, Bethesda, MD, USA) and normalized to GAPDH.

### *2.9 Cell Proliferation Assay*

Proliferation of transfected cells was assessed with the Cell Counting Kit-8 (CCK-8, Dojindo, Mashiki, Kumamoto, Japan) after seeding at a density of $5 \times 10^3$ cells per well in 96-well plates. After 24 hours of culture, following the addition of 10 µL of CCK-8 solution per well, the plates were incubated at 37 °C for 2 hours. The absorbance was measured on a microplate reader at 450 nm, with triplicate measurements performed for each experiment.

### *2.10 Wound Healing Assay*

Cell migratory ability was examined via scratch wound healing assay. Cells were first seeded in 6-well plates and allowed to reach confluence. Cells were cultured to 100% confluence in 6-well plates, scratched with a 200 µL pipette tip, washed with phosphate-buffered saline (PBS) to eliminate detached cells, and then incubated in serum-free medium. Images of wound closure were captured at 0 and 24 hours by inverted microscopy, and wound areas were quantified with Image J software. The migratory capacity was expressed as the percentage reduction in wound area: (initial area – final area) / initial area × 100%.

### *2.11 Apoptosis Assay*

Apoptosis was evaluated using the Annexin V-fluorescein isothiocyanate and propidium iodide kit (BD Biosciences, San Jose, CA, USA). At 48 hours post-transfection and treatment, cells were collected, rinsed with ice-cold PBS, and resuspended in binding buffer. Following a 15-minute staining with Annexin V-fluorescein isothiocyanate and propidium iodide in the dark, flow cytometry was performed using a BD FACSCanto II system. Apoptosis was analyzed by selecting cells in the P1 gate of the scatter plot (**Supplementary Fig. 1**). Cell debris, which appeared in the region with low FSC and SSC in the scatter plot, was excluded. Multicellular particles, often presenting as discrete cell clusters with high FSC values, were also excluded from the P1 gate. Cells stained with Annexin V-FITC indicated apoptotic cells, corresponding to the B525-FITC-A channel. Cells stained with propidium iodide for DNA indicated late-stage dead cells, corresponding to the Y585-PE-A channel. Cells co-stained with Annexin V-FITC and propidium iodide indicated late-stage apoptotic cells (Q1-UR cluster), while cells stained only with Annexin V-FITC indicated early-stage apoptotic cells (Q1-LR cluster).

### *2.12 Statistical Analyses*

All bioinformatics related computations, including differential expression, enrichment, and correlation analyses on Gene Expression Omnibus datasets, were carried out using R software (version 4.1.1, R Foundation for Statistical Computing, Vienna, Austria). For experimental validation, data from IHC, WB, cellular assays, and clinical measurements were analysed and plotted using GraphPad Prism 8 (Version 8.0, GraphPad Software, San Diego, CA, USA). Normality of continuous variables was assessed, and Data are presented as mean ± SD. Between-group comparisons were performed using an independent two-sided Student's *t*-test assuming equal variances (n = 5 per group). To examine the association of placental MFAP5 protein expression with SBP and neonatal birth weight, Pearson's correlation analysis was conducted. A $p$-value < 0.05 was considered statistically significant.

## 3. Results

### *3.1 Identification of DEGs Between Normotensive and PE Placental Tissues*

To identify DEGs between placental tissues from normotensive controls and PE patients, we employed the limma package in R software (Fig. 1A). A total of 155 DEGs from the GSE10588 dataset and 186 DEGs from the GSE44711 dataset were intersected, revealing 10 overlapping genes: *QPCT*, *MFAP5*, *LVRN*, *LEP*, *INHA*, *UCP2*, *HTRA4*, *BHLHE40*, *SERTAD4*, and *TPBG* (Fig. 1B). Among these candidate genes, *MFAP5* has been implicated in the regulation and structural maintenance of the ECM, which has been demonstrated to be associated with the PE pathogenesis [6,7,20]. *MFAP5* was verified through volcano plots in GSE10588 and GSE44711. Consistent with the findings in Fig. 2A, *MFAP5* was highly expressed in the GSE75010 dataset (Fig. 2B).

### *3.2 Interaction Networks of MFAP5*

Analysis of the STRING database identified 22 proteins and interaction networks linked to MFAP5, among which 8 proteins including LOX, LOXL1, LOXL2, LOXL3, LOXL4, MFAP2, JAG1, and NOTCH1, showing the highest confidence correlation (Fig. 3A). Expanded protein interaction analysis using the GeneMANIA database was performed on these 8 proteins, identifying an additional 20 interacting partners, including SCART1, CD163L1, MMP23B, SSC4D, SSC5D, CD5L, CD163, CD6, CD5, EFEMP2, JAG2, HHIPL1, SCARA5, MSR1, MARCO, DLL3, NEURL1, FBN2, NOTCH3, and NOTCH4 (Fig. 3B).

### *3.3 Enrichment Analysis of MFAP5-Related Genes*

GO and KEGG enrichment analyses were performed to investigate the biological functions of MFAP5, based on a gene set consisting of MFAP5 and its 22 interactors (23 genes), identified from the PPI network. GO analysis revealed that MFAP5 was primarily associated with external tissue structure, basement membrane composition, microfibril organization, and ECM composition (Fig. 4A). The results from KEGG pathway enrichment analysis re-

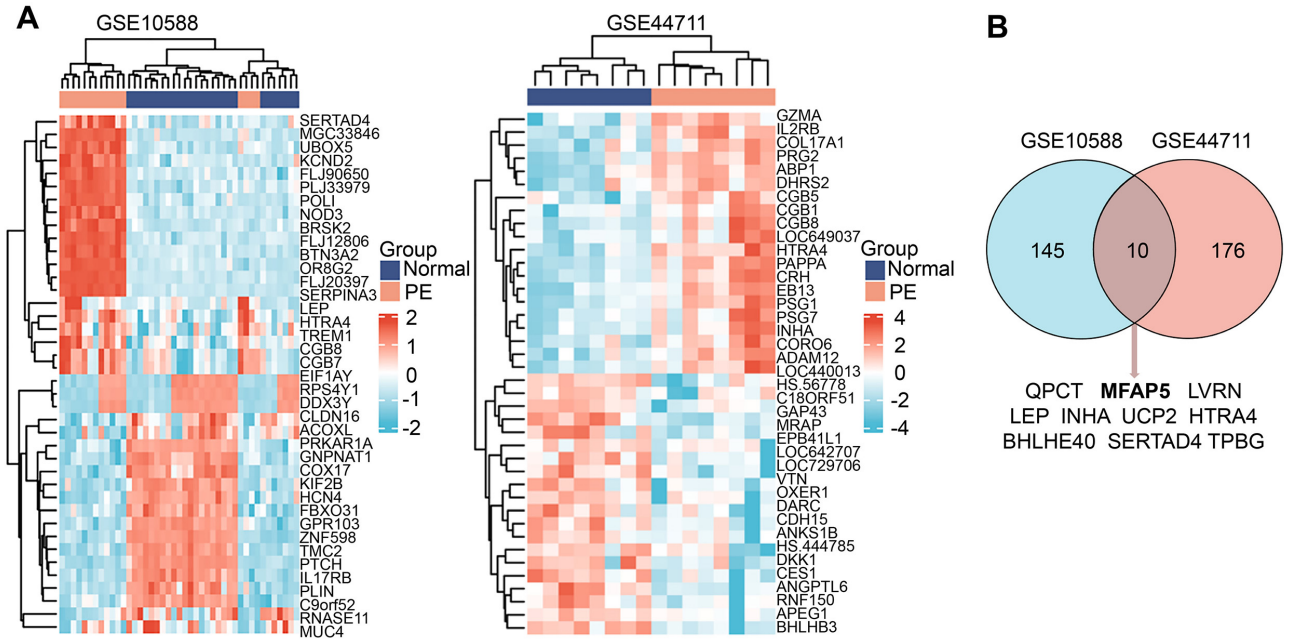



**Fig. 1. Identification of DEGs in preeclampsia placental tissues**. (A) Heatmap visualization of DEGs identified in the GSE10588 and GSE44711 datasets. (B) Venn diagram depicting the overlap between the two DEG datasets and the resulting candidate genes. DEGs, differentially expressed genes; *MFAP5*, microfibril-associated protein 5.

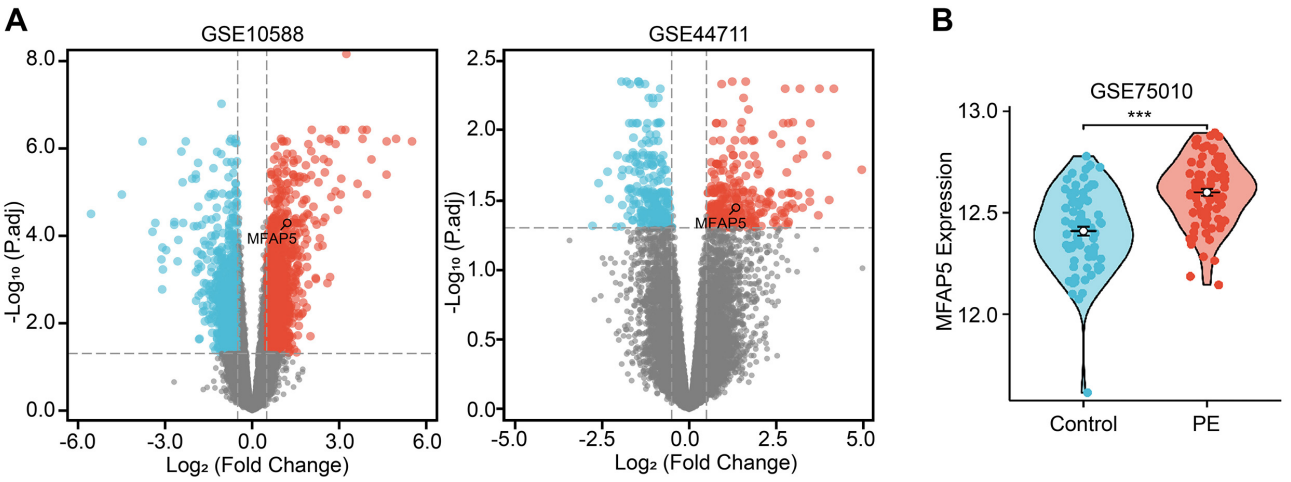



**Fig. 2. Validation of *MFAP5* gene expression**. (A) *MFAP5* expression in the GSE10588 and GSE44711 datasets. (B) MFAP5 expression in the independent validation dataset GSE75010. ***$p < 0.001$; PE, preeclampsia.

vealed MFAP5's implication in multiple oncogenic processes, notably the MAPK and Notch signaling pathways (Fig. 4B). Additionally, these biological functions were further validated through Metascape analysis, which confirmed the associations between cellular composition and both the canonical and non-canonical Notch signaling pathways (Fig. 4C,D).

### *3.4 General Parameters of the Study Subjects*

Clinical information of the participants in the normotensive and PE groups is shown in Table 1. No statistically significant differences were observed regarding maternal age or body mass index (BMI) between the two groups ($p > 0.05$). For the PE group, the average SBP and DBP were recorded as 166.6 ± 10.0 mmHg and 104.2 ± 4.6 mmHg, respectively. By comparison, the average blood pressure values in the normotensive group were 117.0 ± 10.7 mmHg (SBP) and 74.4 ± 7.0 mmHg (DBP). Statistically significant differences were observed in SBP and DBP.. Specifically, neonatal birth weight in the PE group was markedly lower, with a mean of 2430.0 ± 907.3 g, compared with 3540.0 ± 254.1 g in the normotensive pregnancy group, a difference that reached statistical significance ($p < 0.05$).

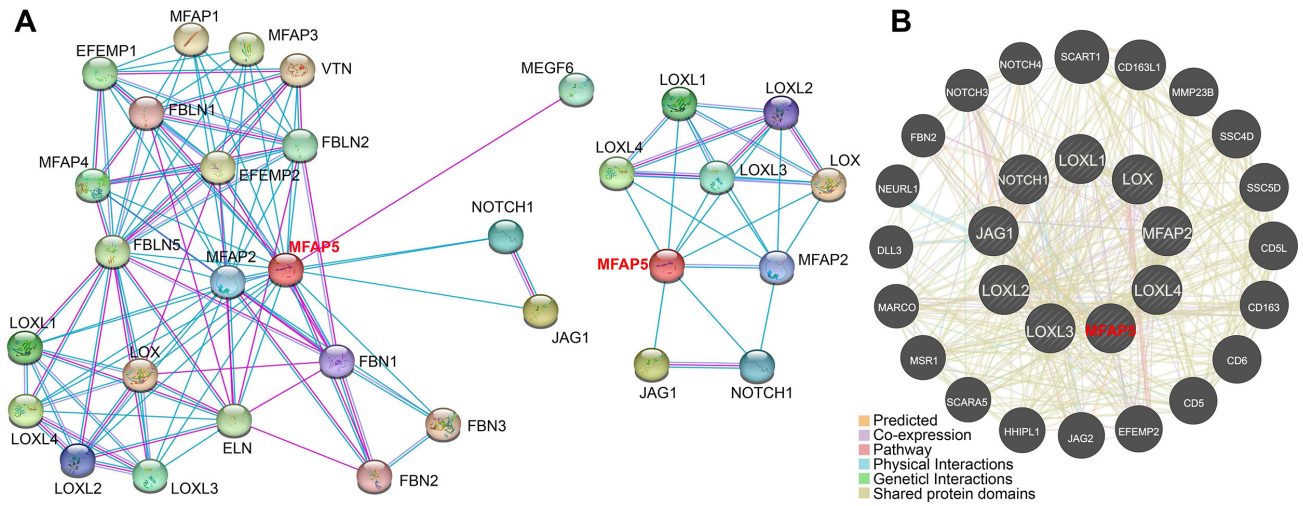



**Fig. 3. MFAP5-related protein-protein interaction analysis in preeclampsia**. (A) The initial network was constructed using a minimum interaction score of 0.150 (low confidence). The core network was extracted using a 0.900 (highest confidence) threshold. (B) GeneMANIA was employed to analyse the 8 core co-expressed genes and the functional roles of hub genes.

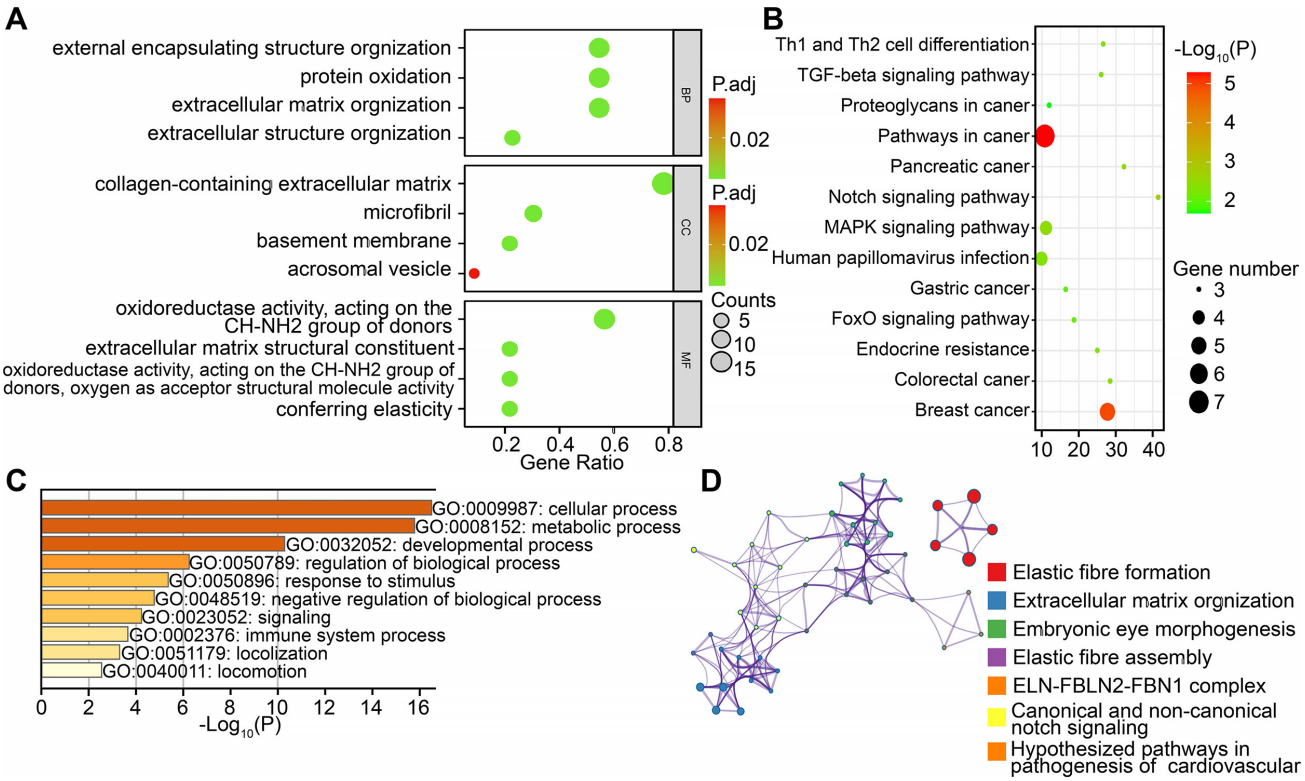



**Fig. 4. GO and KEGG enrichment analysis of MFAP5 in preeclampsia**. (A) GO term enrichment analysis of MFAP5 across BP, CC, and MF, was associated with the extracellular matrix. (B) KEGG pathway enrichment analysis implicated MFAP5 in the Notch signaling pathway. (C) Horizontal bar plot of GO terms associate with MFAP5 and its 22 binding partners (STRING database), with bars colored based on –log$_{10}$($p$) value. (D) Network of enriched terms colored by cluster identifier, with nodes sharing the same identifier clustered together. GO, Gene Ontology; KEGG, Kyoto Encyclopedia of Genes and Genomes; BP, biological process; CC, cellular component; MF, molecular function.

### *3.5 MFAP5 Is Overexpressed in PE Placental Tissues*

MFAP5 expression was evaluated in placental tissues collected from 5 PE patients and 5 normotensive pregnant women respectively using both IHC and WB analyses. IHC staining demonstrated significantly higher MFAP5 expression in PE placental tissues compared with normotensive

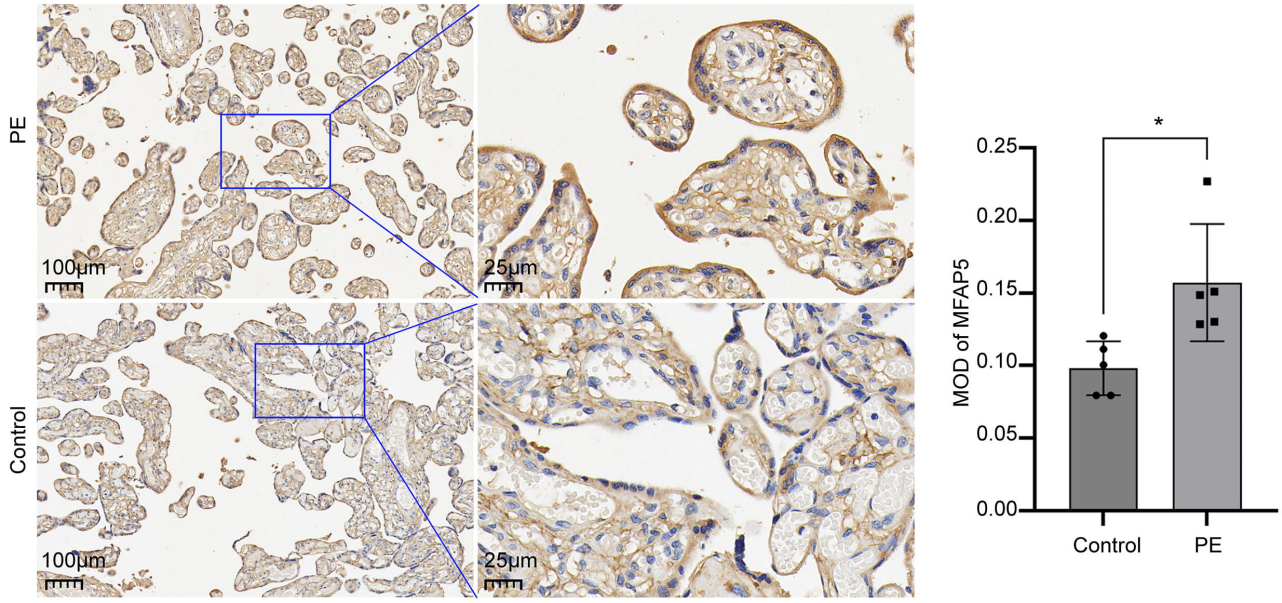



**Fig. 5. Immunohistochemistry of MFAP5 in placental tissues**. MFAP5 expression in preeclampsia versus normotensive placental tissues was assessed by immunohistochemistry (*$p$ = 0.0321).

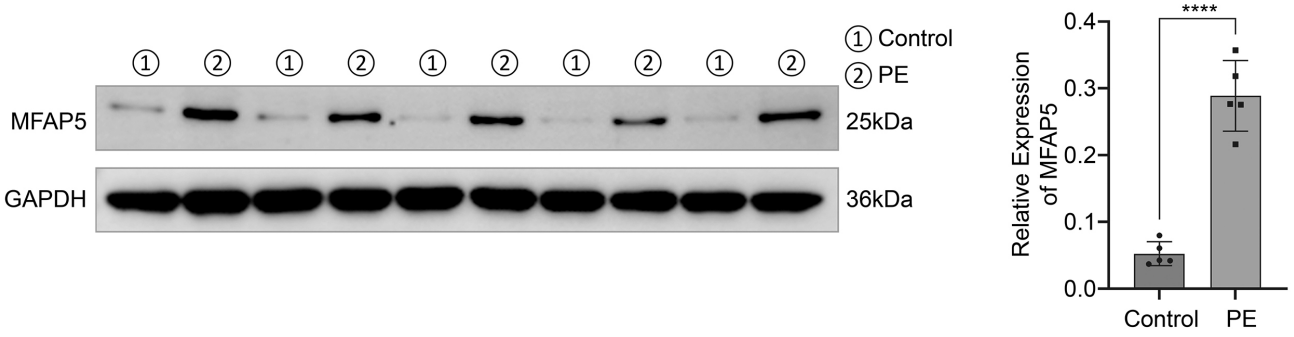



**Fig. 6. MFAP5 protein expression in placental tissues**. Placental MFAP5 expression was evaluated by western blotting in preeclampsia cases and normotensive controls. Control is denoted by ①, and PE by ②, (****$p$ < 0.0001). GAPDH, glyceraldehyde-3-phosphate dehydrogenase.

**Table 1. Comparison of general clinical characteristics between normotensive and PE groups**.

| Clinical parameters | Normal (n = 5) | PE (n = 5) | $p$-value |
|---|---|---|---|
| Age (year) | 32.0 ± 3.5 | 33.6 ± 5.2 | 0.584 |
| BMI (kg/m$^2$) | 24.3 ± 1.9 | 23.1 ± 2.0 | 0.255 |
| SBP (mmHg) | 117.0 ± 10.7 | 166.6 ± 10.0 | <0.001 |
| DBP (mmHg) | 74.4 ± 7.0 | 104.2 ± 4.6 | <0.001 |
| Newborn weight (g) | 3540.0 ± 254.1 | 2430.0 ± 907.3 | 0.030 |

All values are calculated as mean ± SD. BMI, body mass index; PE, preeclampsia; SD, standard deviation; SBP, systolic blood pressure; DBP, diastolic blood pressure.

controls (Fig. 5). Additionally, WB analysis of MFAP5 protein levels in placental tissues from both groups yielded results were consistent with the IHC findings, providing further evidence of significantly elevated MFAP5 expression in PE placental tissues (Fig. 6). In this cohort, placental MFAP5 protein expression correlated positively with SBP ($R^2$ = 0.62, $p$ = 0.007) (**Supplementary Fig. 2**).

### *3.6 MFAP5 Modulates Trophoblast Proliferation, Migration, EMT, and Apoptosis via the Notch Pathway*

To explore MFAP5 function in trophoblasts, gain-of-function experiments were conducted in HTR8/SVneo cells. Cells were transfected with an MFAP5 overexpression plasmid, with or without subsequent DAPT treatment to inhibit Notch signaling. Successful MFAP5 overexpression was confirmed by RT-qPCR and WB (Fig. 7A).

Cell proliferation and migration were markedly inhibited by MFAP5 overexpression. According to CCK-8 analysis, cell viability was significantly lower in the OE-MFAP5 group than in the OE-NC group at 24 h, and DAPT treatment further exacerbated this decrease (Fig. 7B). As demonstrated by wound healing assay, MFAP5

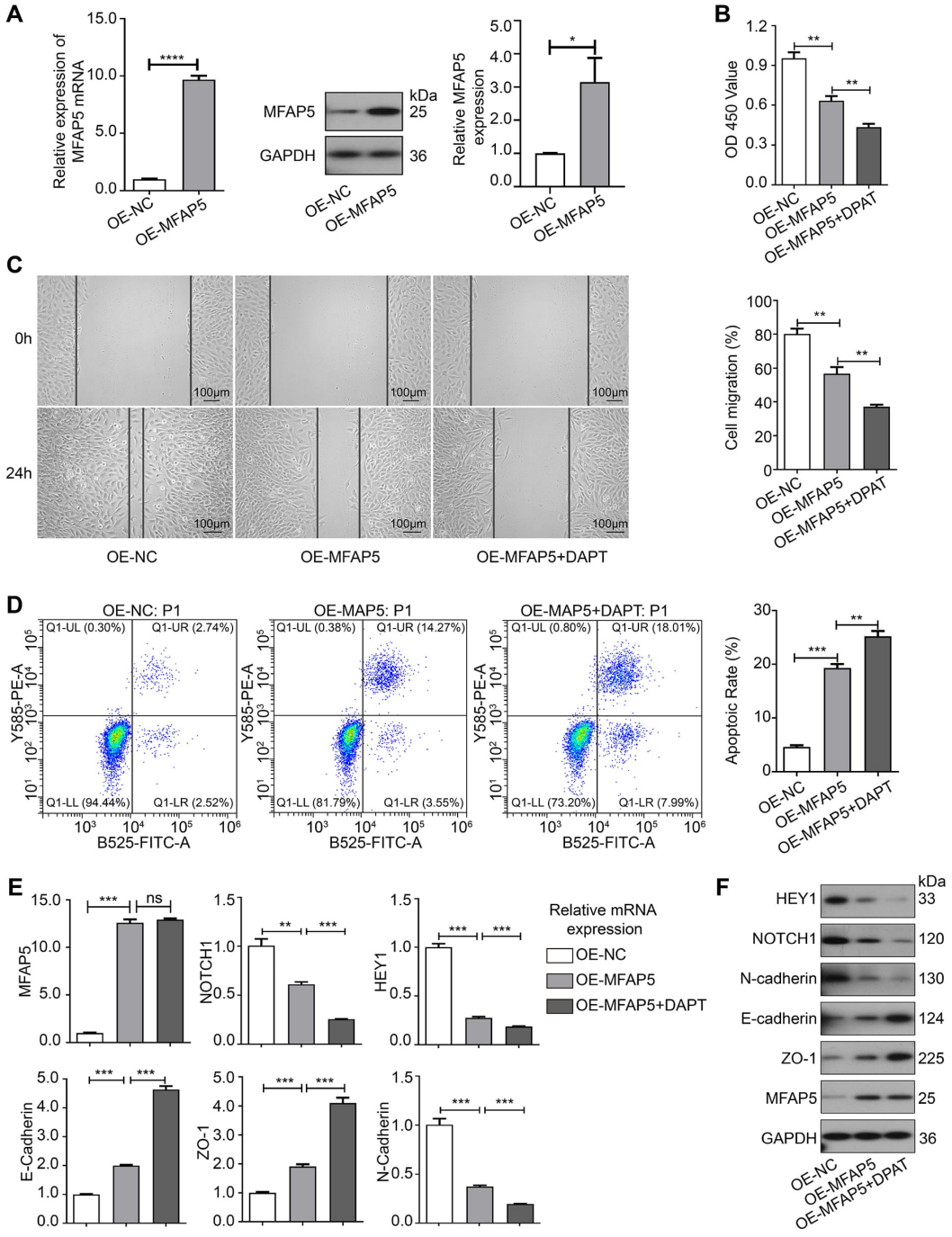



**Fig. 7. MFAP5 suppresses HTR8/SVneo cells proliferation, migration, and EMT while promoting apoptosis via Notch signaling**. (A) MFAP5 expression in OE-NC and OE-MFAP5 cells: mRNA (left) and protein (right) levels determined by RT-qPCR and WB, respectively. (B) Compared with the OE-NC group, MFAP5 overexpression led to a significant decrease in cell viability at 24 h, an effect that was further potentiated by DAPT treatment. (C) Wound healing assay showing cell migration at 0 h and 24 h. Quantification of the wound closure percentage is presented on the right. (D) Apoptosis detected by flow cytometry in OE-NC, OE-MFAP5, and OE-MFAP5 + DAPT groups. Representative dot plots (top) and quantification of apoptotic rate (bottom) are shown. (E) Relative mRNA expression levels of MFAP5, N-cadherin, E-cadherin, ZO-1, Hey1, and NOTCH1 in the indicated groups, as determined by RT-qPCR. (F) Notch pathway components and EMT markers detected by WB. WB data analysis is presented in the **Supplementary Fig. 3**. All data are reported as mean ± SD. Significance levels: *$p < 0.05$, **$p < 0.01$, ***$p < 0.001$, ****$p < 0.0001$; ns, not significant; EMT, epithelial-mesenchymal transition; WB, western blotting; RT-qPCR, reverse transcription quantitative PCR; OE-NC, overexpression-negative control; DAPT, N-[N-(3,5-Difluorophenacetyl)-L-alanyl]-S-phenylglycine t-butyl ester; ZO-1, zonula occludens-1; Hey1, hairy/enhancer-of-split related with YRPW motif 1; NOTCH1, Notch receptor 1.


IMR Press

overexpression significantly impaired cell migration, with DAPT treatment further enhancing this suppressive effect (Fig. 7C).

MFAP5 overexpression induces apoptosis. Flow cytometry analysis demonstrated that the apoptotic rate was significantly higher in OE-MFAP5 cells than in OE-NC cells, and DAPT treatment further increased MFAP5-induced apoptosis (Fig. 7D).

MFAP5 regulates Notch signaling and EMT markers. WB analysis showed that MFAP5 overexpression downregulated Notch1 and its downstream effector Hey1, indicating suppression of the Notch pathway. Concomitantly, increased expression of E-cadherin and ZO-1, as well as decreased N-cadherin expression pointed to EMT inhibition. DAPT treatment, which inhibits Notch signaling, amplified the effects of MFAP5 on these markers, leading to more pronounced downregulation of Notch1, Hey1, and N-cadherin, as well as upregulation of E-cadherin and ZO-1 (Fig. 7E,F). Together, these results suggest that MFAP5 suppresses trophoblast proliferation, migration, and EMT while promoting apoptosis via Notch pathway inhibition, and that pharmacological Notch blockade with DAPT further enhances these outcomes.

## 4. Discussion

The present study investigated the expression and potential functional role of MFAP5 in PE. The principal findings are fourfold. First, bioinformatics screening and independent dataset validation identified MFAP5 as a consistently upregulated gene in PE placental tissues. Second, *in silico* analyses linked MFAP5 to ECM organization and the Notch signaling pathway. Third, preliminary histological validation confirmed elevated MFAP5 protein expression in a small-scale pilot cohort of PE placental tissues. Fourth, and most importantly, functional assays in HTR8/SVneo trophoblast cells demonstrated that MFAP5 overexpression significantly suppressed cell proliferation, migration, and EMT, while promoting apoptosis. Overall, these findings implicate MFAP5 in the defective trophoblast invasion and placental dysfunction characteristic of PE.

PE is a complex pregnancy complication involving multiple pathogenic factors, yet the mechanisms underlying its pathophysiology remain poorly understood [21]. Although the precise etiology of PE has not been established, the placenta is recognized as playing a pivotal role in its development and progression. In recent years, the incidence of PE has been rising continuously, posing significant risks to maternal and neonatal health [22]. Nevertheless, reliable biomarkers for predicting PE onset are still lacking [23], and the identification of key predictive markers for PE has become an urgent clinical priority.

The placenta is the principal mediator of the maternal-fetal exchange, critically regulating *in utero* development and thereby influencing both fetal growth and future health [24,25,26]. Although the placenta is a central organ of reproduction and a master regulator of fetal growth, it is often excluded from comprehensive omics analyses, limiting insights into its essential evolutionary and developmental roles [27]. Recent studies have identified placental factors, including sFlt-1 and PlGF, as useful tools for early PE prediction. However, their clinical utility may be further optimized, as predictive performance varies across gestational stages [28]. Through DEGs analysis and preliminary experimental validation, we identified MFAP5 as a highly expressed molecule in placental tissues of the PE group. To the best of our knowledge, only Hu et al. [8] have previously reported MFAP5 as a hub gene involved in M1 macrophage infiltration in PE. To date, no study has examined the expression or functional significance of MFAP5 in the PE placenta. Therefore, the present findings add new evidence supporting its involvement in the pathogenesis of PE.

MFAP5, a multifunctional protein secreted by mesenchymal cells, is also referred to as microfibril-associated glycoprotein 2. It is critically involved in elastic microfibril assembly, tissue development, endothelial cell behavior, and immune regulation [29]. In papillary thyroid cancer, MFAP5 overexpression suppresses tumor progression and aerobic glycolysis via the EFEMP2/Wnt/β-Catenin axis, while in endometrial cancer cells, it impairs EMT through inhibition of the AKT/mTOR pathway [30,31]. In contrast, MFAP5 overexpression in cancer-associated fibroblast has been reported to promote tumorigenesis and metastasis through EMT in gastric and bladder cancers [32,33,34]. Despite its well-established involvement in cancer cell proliferation and metastasis, the role of MFAP5 in pregnancy disorders remains poorly understood. Consistent with our STRING analysis findings, previous studies have also demonstrated that several MFAP5-interacting proteins, including LOX, LOXL2, JAG1, and CD16, are involved in the pathogenesis of PE [35,36,37,38,39,40,41]. These convergent findings strongly suggest that MFAP5 is integrated into signaling networks central to placental dysfunction, underscoring its potential role in the development of PE.

Based on our enrichment analysis results and the existing literature, we propose an integrated mechanistic hypothesis for the role of MFAP5 in PE pathogenesis. We hypothesize that MFAP5 contributes to defective placentation by acting at the nexus of ECM remodeling and the Notch signaling pathway, ultimately impairing trophoblast EMT and invasion. The ECM, a primary mechanosignaling hub, is critical for trophoblast differentiation and invasion [42,43]. E-cadherin and N-cadherin, two classic EMT markers, are implicated in the regulation of trophoblast invasion [44]. EMT drives the differentiation of cytotrophoblasts into EVTs, facilitating their acquisition of the invasive phenotype essential for placental development [5,45]. Impaired EMT and reduced trophoblast invasion are hallmarks of PE. The GO analysis in the present study

indicated a strong association between MFAP5 and ECM composition and basement membrane organization. We hypothesize that MFAP5 upregulation in the PE placenta may alter the local ECM microenvironment, increase stromal stiffness, or disrupt instructive signals necessary for normal trophoblast function. KEGG analysis also implicated MFAP5 in the Notch signaling pathway, which plays an essential role in controlling cell fate, differentiation, and invasion. The Notch pathway is active during placentation, and its dysregulation has been linked to PE [46]. Previous reports indicate that the Notch signaling pathway promotes EMT in various cancers [9,47]. Our findings are consistent with those of Perlman et al. [38], who demonstrated that JAG1 expression was markedly reduced in placental tissues from patients with severe PE, resulting in impaired trophoblast migration and implicating Notch signaling in hypoxia-induced PE. Moreover, hypoxia, a hallmark of the PE placenta, has been shown to induce MFAP5 expression in tumor models [32,48]. In our cellular model, MFAP5 overexpression was associated with decreased Notch pathway activity, evidenced by reduced NOTCH1 and Hey1 expression, and a shift in EMT marker expression characterized by decreased N-cadherin and increased E-cadherin. These results suggest that MFAP5 may restrain trophoblast EMT and invasiveness at least partly through modulation of Notch signaling.

*Limitations*

Despite these insights, several limitations warrant consideration. First, although the histological findings reached statistical significance, they should be interpreted as preliminary due to the limited sample size (n = 5 per group). Second, the observed differences may be influenced by gestational age; future studies should therefore control for this variable using larger, well-characterized, gestational age-matched cohorts to confirm the clinical relevance of MFAP5 upregulation. Third, while the *in vitro* experiments presented here provide the first functional evidence linking MFAP5 to trophoblast dysfunction, the precise molecular mechanisms, including the upstream regulators of MFAP5 and its direct interacting partners in trophoblasts, remain to be elucidated. The HTR8/SVneo line (first-trimester EVTs) and our placental tissues (third-trimester, mixed trophoblast subtypes) differ in cell type and stage, limiting translatability. Validation using stage-matched primary cells is needed. Finally, the absence of *in vivo* validation using PE animal models represents a critical gap, as such validation is essential for establishing causality. Therefore, while the *in vitro* findings presented here strongly support a mechanistic role for MFAP5 in trophoblast dysfunction, *in vivo* studies are necessary to confirm causality in PE pathogenesis.

## 5. Conclusions

Collectively, these findings identify MFAP5 as a novel upregulated marker in PE placentas and provide the first evidence that it suppresses trophoblast proliferation, migration, and EMT while promoting apoptosis, likely through disruption of Notch signaling. Taken together, these findings support MFAP5 as a potential pathogenic factor and a candidate biomarker for PE, warranting further clinical validation. To further elucidate its clinical relevance, future work should focus on: (1) validating MFAP5 protein expression in large-scale, multicenter cohorts with rigorous clinical phenotyping; (2) defining the precise molecular mechanisms underlying MFAP5-mediated inhibition of trophoblast function; (3) exploring the translational potential of MFAP5-directed intervention in preclinical PE models; and (4) determining whether circulating MFAP5 levels in maternal blood can serve as a non-invasive candidate biomarker requiring further validation for early prediction or monitoring of PE.

## Availability of Data and Materials

The datasets generated and analyzed during the current study are not publicly available due to patient confidentiality and institutional regulations, but are available from the corresponding author on reasonable request.

## Author Contributions

JS and YZ: conceptualization, study design, methodology, data curation, formal analysis, and writing original draft preparation. ZJW: conceptualization, revised the manuscript. All authors contributed to the revision, approved the final manuscript, and are accountable for all aspects of the work.

## Ethics Approval and Consent to Participate

This study adhered to the principles of the Declaration of Helsinki. Approval was granted by the Ethics Committee of the Central Hospital of Wuhan (No. WHZXKYL2023-134), and written informed consent was obtained from all participants.


## Acknowledgment

We extend our thanks to Dr. Kecheng Huang (Department of Obstetrics and Gynecology, Tongji Hospital, Tongji Medical College, Huazhong University of Science and Technology, Wuhan, China) and Dr. Yanxing Wei, (Department of Obstetrics and Gynecology, Nanfang Hospital, Southern Medical University, Guangzhou, China) for their insightful contributions and advice.

## Funding

Financial support for this work was provided by the Natural Science Foundation of Hubei Province (2021CFB526).


## Conflicts of Interest

The authors declare no conflicts of interest.

## Supplementary Material

Supplementary material associated with this article can be found, in the online version, at https://doi.org/10.31083/CEOG48528.

## References


[1] Ives CW, Sinkey R, Rajapreyar I, Tita ATN, Oparil S. Preeclampsia-Pathophysiology and Clinical Presentations: JACC State-of-the-Art Review. Journal of the American College of Cardiology. 2020; 76: 1690–1702. https://doi.org/10.1016/j.jacc.2020.08.014

[2] Zakiyah N, Postma MJ, Baker PN, van Asselt ADI, IMPROvED Consortium. Pre-eclampsia Diagnosis and Treatment Options: A Review of Published Economic Assessments. PharmacoEconomics. 2015; 33: 1069–1082. https://doi.org/10.1007/s40273-015-0291-x

[3] Sheridan MA, Fernando RC, Gardner L, Hollinshead MS, Burton GJ, Moffett A, et al. Establishment and differentiation of long-term trophoblast organoid cultures from the human placenta. Nature Protocols. 2020; 15: 3441–3463. https://doi.org/10.1038/s41596-020-0381-x

[4] Torres-Torres J, Espino-Y-Sosa S, Martinez-Portilla R, Borboa-Olivares H, Estrada-Gutierrez G, Acevedo-Gallegos S, et al. A Narrative Review on the Pathophysiology of Preeclampsia. International Journal of Molecular Sciences. 2024; 25: 7569. https://doi.org/10.3390/ijms25147569

[5] E Davies J, Pollheimer J, Yong HEJ, Kokkinos MI, Kalionis B, Knöfler M, et al. Epithelial-mesenchymal transition during extravillous trophoblast differentiation. Cell Adhesion & Migration. 2016; 10: 310–321. https://doi.org/10.1080/19336918.2016.1170258

[6] Wang X, Zhang Q, Ren Y, Liu C, Gao H. Research Progress on Extracellular Matrix Involved in the Development of Preeclampsia. Current Protein & Peptide Science. 2024; 25: 527–538. https://doi.org/10.2174/0113892037284176240302052521

[7] Hu H, Ma J, Li Z, Ding Z, Chen W, Peng Y, et al. CyPA interacts with SERPINH1 to promote extracellular matrix production and inhibit epithelial-mesenchymal transition of trophoblast via enhancing TGF-β/Smad3 pathway in preeclampsia. Molecular and Cellular Endocrinology. 2022; 548: 111614. https://doi.org/10.1016/j.mce.2022.111614

[8] Hu P, Luo S, Qu G, Luo Q, Tian Y, Huang K, et al. Identification and validation of feature genes associated with M1 macrophages in preeclampsia. Aging. 2023; 15: 13822–13839. https://doi.org/10.18632/aging.205264

[9] Chen Z, Yan X, Li K, Ling Y, Kang H. Stromal fibroblast-derived MFAP5 promotes the invasion and migration of breast cancer cells via Notch1/slug signaling. Clinical & Translational Oncology: Official Publication of the Federation of Spanish Oncology Societies and of the National Cancer Institute of Mexico. 2020; 22: 522–531. https://doi.org/10.1007/s12094-019-02156-1

[10] Derisoud E, Jiang H, Zhao A, Chavatte-Palmer P, Deng Q. Revealing the molecular landscape of human placenta: a systematic review and meta-analysis of single-cell RNA sequencing studies. Human Reproduction Update. 2024; 30: 410–441. https://doi.org/10.1093/humupd/dmae006

[11] Barrett T, Wilhite SE, Ledoux P, Evangelista C, Kim IF, Tomashevsky M, et al. NCBI GEO: archive for functional genomics data sets--update. Nucleic Acids Research. 2013; 41: D991–D995. https://doi.org/10.1093/nar/gks1193

[12] Chang KJ, Seow KM, Chen KH. Preeclampsia: Recent Advances in Predicting, Preventing, and Managing the Maternal and Fetal Life-Threatening Condition. International Journal of Environmental Research and Public Health. 2023; 20: 2994. https://doi.org/10.3390/ijerph20042994

[13] Szklarczyk D, Kirsch R, Koutrouli M, Nastou K, Mehryary F, Hachilif R, et al. The STRING database in 2023: protein-protein association networks and functional enrichment analyses for any sequenced genome of interest. Nucleic Acids Research. 2023; 51: D638–D646. https://doi.org/10.1093/nar/gkac1000

[14] Franz M, Rodriguez H, Lopes C, Zuberi K, Montojo J, Bader GD, et al. GeneMANIA update 2018. Nucleic Acids Research. 2018; 46: W60–W64. https://doi.org/10.1093/nar/gky311

[15] Zhou Y, Zhou B, Pache L, Chang M, Khodabakhshi AH, Tanaseichuk O, et al. Metascape provides a biologist-oriented resource for the analysis of systems-level datasets. Nature Communications. 2019; 10: 1523. https://doi.org/10.1038/s41467-019-09234-6

[16] Xu Y, Sui L, Qiu B, Yin X, Liu J, Zhang X. ANXA4 promotes trophoblast invasion via the PI3K/Akt/eNOS pathway in preeclampsia. American Journal of Physiology. Cell Physiology. 2019; 316: C481–C491. https://doi.org/10.1152/ajpcell.00404.2018

[17] Wu Z, Wang T, Fang M, Huang W, Sun Z, Xiao J, et al. MFAP5 promotes tumor progression and bone metastasis by regulating ERK/MMP signaling pathways in breast cancer. Biochemical and Biophysical Research Communications. 2018; 498: 495–501. https://doi.org/10.1016/j.bbrc.2018.03.007

[18] Zhao R, Zhou Y, Shi H, Ye W, Lyu Y, Zhang W, et al. Effect of Gestational Diabetes on Postpartum Depression-like Behavior in Rats and Its Mechanism. Nutrients. 2022; 14: 1229. https://doi.org/10.3390/nu14061229

[19] Schmittgen TD, Livak KJ. Analyzing real-time PCR data by the comparative C(T) method. Nature protocols. 2008; 3: 1101–1108. https://doi.org/10.1038/nprot.2008.73

[20] Shi JW, Lai ZZ, Yang HL, Yang SL, Wang CJ, Ao D, et al. Collagen at the maternal-fetal interface in human pregnancy. International Journal of Biological Sciences. 2020; 16: 2220–2234. https://doi.org/10.7150/ijbs.45586

[21] Rana S, Lemoine E, Granger JP, Karumanchi SA. Preeclampsia: Pathophysiology, Challenges, and Perspectives. Circulation Research. 2019; 124: 1094–1112. https://doi.org/10.1161/CIRCRESAHA.118.313276

[22] Rosenberg EA, Seely EW. Update on Preeclampsia and Hypertensive Disorders of Pregnancy. Endocrinology and Metabolism Clinics of North America. 2024; 53: 377–389. https://doi.org/10.1016/j.ecl.2024.05.012

[23] Chiang YT, Seow KM, Chen KH. The Pathophysiological, Genetic, and Hormonal Changes in Preeclampsia: A Systematic Review of the Molecular Mechanisms. International Journal of Molecular Sciences. 2024; 25: 4532. https://doi.org/10.3390/ijms25084532

[24] Colson A, Sonveaux P, Debiève F, Sferruzzi-Perri AN. Adaptations of the human placenta to hypoxia: opportunities for interventions in fetal growth restriction. Human Reproduction Update. 2021; 27: 531–569. https://doi.org/10.1093/humupd/dmaa053

[25] Aplin JD, Myers JE, Timms K, Westwood M. Tracking placental development in health and disease. Nature Reviews. Endocrinology. 2020; 16: 479–494. https://doi.org/10.1038/s41574-020-0372-6

[26] Cindrova-Davies T, Sferruzzi-Perri AN. Human placental development and function. Seminars in Cell & Developmental Biology. 2022; 131: 66–77. https://doi.org/10.1016/j.semcdb.2022.03.039

[27] Gong S, Gaccioli F, Dopierala J, Sovio U, Cook E, Volders PJ, et al. The RNA landscape of the human placenta in health and disease. Nature Communications. 2021; 12: 2639. https://doi.org/10.1038/s41467-021-22695-y

[28] Jena MK, Sharma NR, Petitt M, Maulik D, Nayak NR. Patho-

genesis of Preeclampsia and Therapeutic Approaches Targeting the Placenta. Biomolecules. 2020; 10: 953. https://doi.org/10.3390/biom10060953

[29] Combs MD, Knutsen RH, Broekelmann TJ, Toennies HM, Brett TJ, Miller CA, et al. Microfibril-associated glycoprotein 2 (MAGP2) loss of function has pleiotropic effects in vivo. The Journal of Biological Chemistry. 2013; 288: 28869–28880. https://doi.org/10.1074/jbc.M113.497727

[30] Sun Y, Dong J, Li J, Zhang Y, Han Y. Overexpression of MFAP5 inhibits the progression of papillary thyroid cancer and aerobic glycolysis by regulating the EFEMP2/Wnt/β-catenin pathway. Pathology, Research and Practice. 2025; 268: 155846. https://doi.org/10.1016/j.prp.2025.155846

[31] Liang G, Qi Z, Du C. MFAP5 inhibits the malignant progression of endometrial cancer cells *in vitro*. Open Life Sciences. 2024; 19: 20220990. https://doi.org/10.1515/biol-2022-0990

[32] Zhang Z, Liang Z, Li D, Wang L, Chen Y, Liang Y, et al. Development of a CAFs-related gene signature to predict survival and drug response in bladder cancer. Human Cell. 2022; 35: 649–664. https://doi.org/10.1007/s13577-022-00673-w

[33] Gao B, Gou X, Feng C, Zhang Y, Gu H, Chai F, et al. Identification of cancer-associated fibrolast subtypes and distinctive role of MFAP5 in CT-detected extramural venous invasion in gastric cancer. Translational Oncology. 2025; 51: 102188. https://doi.org/10.1016/j.tranon.2024.102188

[34] Shi Y, E J, Wu X, Wang F. Upregulation of MFAP5 Enhances COL1A1 Expression, Promoting Epithelial-Mesenchymal Transition in Gastric Cancer Cells. Discovery Medicine. 2024; 36: 2079–2087. https://doi.org/10.24976/Discov.Med.202436189.192

[35] Xu XH, Jia Y, Zhou X, Xie D, Huang X, Jia L, et al. Down-regulation of lysyl oxidase and lysyl oxidase-like protein 2 suppressed the migration and invasion of trophoblasts by activating the TGF-β/collagen pathway in preeclampsia. Experimental & Molecular Medicine. 2019; 51: 1–12. https://doi.org/10.1038/s12276-019-0211-9

[36] Xu XH, Tang LC, Hao F, Jin LP. Upregulation of miR-29a suppressed the migration and invasion of trophoblasts by directly targeting LOXL2 in preeclampsia. Journal of Hypertension. 2021; 39: 1642–1651. https://doi.org/10.1097/HJH.0000000000002837

[37] Levin HI, Sullivan-Pyke CS, Papaioannou VE, Wapner RJ, Kitajewski JK, Shawber CJ, et al. Dynamic maternal and fetal Notch activity and expression in placentation. Placenta. 2017; 55: 5–12. https://doi.org/10.1016/j.placenta.2017.04.014

[38] Perlman BE, Merriam AA, Lemenze A, Zhao Q, Begum S, Nair M, et al. Implications for preeclampsia: hypoxia-induced Notch promotes trophoblast migration. Reproduction (Cambridge, England). 2021; 161: 681–696. https://doi.org/10.1530/REP-20-0483

[39] Shen J, Hu N, Wang Z, Yang L, Chen R, Zhang L, et al. Ghrelin alleviates placental dysfunction by down-regulating NF-κB phosphorylation in LPS-induced rat model of preeclampsia. European Journal of Pharmacology. 2024; 972: 176569. https://doi.org/10.1016/j.ejphar.2024.176569

[40] Gong F, Wang J, Lu N, Wang J, Wang J, Shi X, et al. The imbalance of circulating monocyte subgroups with a higher proportion of the CD14+CD16+CD163+ phenotype in patients with preeclampsia. Immunology Letters. 2023; 253: 1–7. https://doi.org/10.1016/j.imlet.2022.11.005

[41] Vishnyakova P, Kuznetsova M, Poltavets A, Fomina M, Kiseleva V, Muminova K, et al. Distinct gene expression patterns for CD14++ and CD16++ monocytes in preeclampsia. Scientific Reports. 2022; 12: 15469. https://doi.org/10.1038/s41598-022-19847-5

[42] Choudhury J, Pandey D, Chaturvedi PK, Gupta S. Epigenetic regulation of epithelial to mesenchymal transition: a trophoblast perspective. Molecular Human Reproduction. 2022; 28: gaac013. https://doi.org/10.1093/molehr/gaac013

[43] Tian H, Shi H, Yu J, Ge S, Ruan J. Biophysics Role and Biomimetic Culture Systems of ECM Stiffness in Cancer EMT. Global Challenges (Hoboken, NJ). 2022; 6: 2100094. https://doi.org/10.1002/gch2.202100094

[44] Blechschmidt K, Mylonas I, Mayr D, Schiessl B, Schulze S, Becker KF, et al. Expression of E-cadherin and its repressor snail in placental tissue of normal, preeclamptic and HELLP pregnancies. Virchows Archiv: an International Journal of Pathology. 2007; 450: 195–202. https://doi.org/10.1007/s00428-006-0343-x

[45] Ackerman Iv WE, Rigo MM, DaSilva-Arnold SC, Do C, Tariq M, Salas M, et al. Epigenetic Changes Regulating Epithelial-Mesenchymal Plasticity in Human Trophoblast Differentiation. Cells. 2025; 14: 970. https://doi.org/10.3390/cells14130970

[46] Ou Y, Zhu L, Wei X, Bai S, Chen M, Chen H, et al. Circular RNA circ_0111277 attenuates human trophoblast cell invasion and migration by regulating miR-494/HTRA1/Notch-1 signal pathway in pre-eclampsia. Cell Death & Disease. 2020; 11: 479. https://doi.org/10.1038/s41419-020-2679-6

[47] Yang X, Bai Q, Chen W, Liang J, Wang F, Gu W, et al. $m^6$ A-Dependent Modulation via IGF2BP3/MCM5/Notch Axis Promotes Partial EMT and LUAD Metastasis. Advanced Science (Weinheim, Baden-Wurttemberg, Germany). 2023; 10: e2206744. https://doi.org/10.1002/advs.202206744

[48] Xu Q, Chang H, Tian X, Lou C, Ma H, Yang X. Hypoxia-induced MFAP5 Promotes Tumor Migration and Invasion via AKT Pathway in Head and Neck Squamous Cell Carcinoma. Journal of Cancer. 2020; 11: 1596–1605. https://doi.org/10.7150/jca.38217